

# Flax-Fabric-Reinforced Arylated Soy Protein Composites: Brittle-Matrix Behavior

Rakesh Kumar,<sup>1</sup> Rajesh D. Anandjiwala<sup>1,2</sup>

<sup>1</sup>Council of Scientific and Industrial Research Materials Science and Manufacturing, Port Elizabeth, South Africa

<sup>2</sup>Department of Textile Science, Faculty of Science, Nelson Mandela Metropolitan University, South Africa

Received 3 June 2011; accepted 27 July 2011

DOI 10.1002/app.35374

Published online 3 November 2011 in Wiley Online Library (wileyonlinelibrary.com).

**ABSTRACT:** Biocomposites were successfully prepared by the reinforcement of soy protein isolate (SPI) with different weight fractions of woven flax fabric. The flax-fabric-reinforced SPI-based composites were then arylated with 2,2-diphenyl-2-hydroxyethanoic acid (DPHEAc) for 4 h to obtain arylated biocomposites. A new method was proposed to determine the amount of carbon dioxide evolved during the arylation of the soy protein in the presence of DPHEAc. Characterizations of the arylated and nonarylated biocomposites were done by Fourier transform infrared spectroscopy, thermogravimetric analysis, and dynamic mechanical thermal analysis. The results indicate that the arylated soy-protein-based composites

exhibited mechanical behavior like brittle-matrix composites, which differentiated them from nonarylated soy-protein-based composites, which showed mechanical behavior similar to polymer-matrix composites. In the arylated composites, there was clear evidence of a stick-slip mechanism, which perhaps dominated and, therefore, prevented easy deformation of the reinforced film. Scanning electron microscopy studies revealed cracks in the arylated soy protein composites when they were subjected to tensile tests. © 2011 Wiley Periodicals, Inc. *J Appl Polym Sci* 124: 3132–3141, 2012

**Key words:** biopolymers; brittle; fibers

## INTRODUCTION

Composites include a wide variety of materials that can be tailored to desired properties for intended end-use applications. In past decades, many efforts have been made to investigate the suitability of natural fibers as reinforcing components for soy-protein-based biopolymers.<sup>1–6</sup>

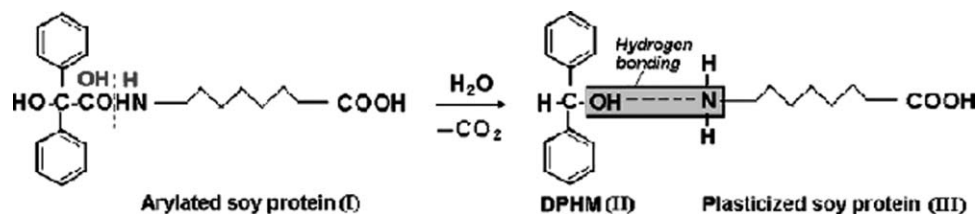
Brittle-matrix composites result from a combination of constituent brittle materials and ultimately may result in materials that are no longer brittle but instead damage-tolerant. These kinds of materials are of interest for thermostructural applications.<sup>7</sup> In brittle-matrix composites, the matrix is less resistant to impact than the fibers. Integrity in these classes of composites is often maintained by fibers, which provide strength to the material. It has been reported that cracking is the main cause of the damage in brittle-matrix composites. In the past, structures or materials of brittle-matrix composites have been designed by the modeling of their mechanical behavior.<sup>8,9</sup>

Typical tensile stress/strain curves of brittle-matrix composites can be grouped by two main charac-

teristics, that is, damage-insensitive and damage-sensitive. Damage-insensitive stress-strain behavior is observed when the deformation of the composites is dominated by fibers with a high modulus, and the matrix, with a relatively low modulus, does not offer perceptible resistance to the deformations. On the other hand, damage-sensitive stress-strain behavior is obtained when the load-carrying contribution of the matrix is dominant.<sup>7</sup>

The modulus of a natural fiber bundle varies between 650 and 1050 MPa.<sup>10</sup> Soy protein films prepared by the solution-casting method show modulus values of 20–50 MPa,<sup>11</sup> whereas soy protein films are prepared at compression-molding ranges from 50 to 100 MPa<sup>1,12–14</sup> under a high relative humidity (RH; 50–75%). Hence, the modulus of soy-protein-based films is very low compared to that of natural fibers. Recently, it has been reported that the arylation of soy protein in the presence of 2,2-diphenyl-2-hydroxyethanoic acid (DPHEAc) leads to a material with a very high modulus, in the range of 800–1100 MPa,<sup>15–17</sup> even under high RHs (50–75% RH). Water-mediated arylation by a dip-coating method is responsible for the increase in the modulus of the soy protein material. This is attributed to the evolution of CO<sub>2</sub> and the formation of a more stable compound, such as 2,2-diphenyl-2-hydroxyl methane (DPHM), from DPHEAc, as shown in the following chemical reaction:<sup>15,16</sup>

Correspondence to: R. Kumar (krrakesh72@gmail.com).



Recently, composites prepared by arylated soy protein reinforced with aligned ramie fiber were also reported.<sup>18</sup> In this article, we report on damage-sensitive composites prepared from arylated soy protein (as the brittle matrix) and flax fabric. The aim of this study was to prepare brittle-matrix composite sheets for sandwich panels with brittle-matrix composite faces for building applications. The loss of CO<sub>2</sub> during the arylation process was quantitatively estimated. The composites were characterized by their mechanical, thermal, thermomechanical, and water uptake properties. The morphology of the arylated composites was also evaluated to determine the presence of cracks and confirm the brittle-matrix behavior.

## EXPERIMENTAL

### Materials

Soy protein isolate (SPI) containing 90.27% protein on a dry basis was purchased from Zhengzhou Rui-kang Enterprise Co., Ltd. (Zhengzhou, China). Thiodiglycol (TDG; bp = 164–166°C, molecular weight = 122.19, and density = 1.182 g/cm<sup>3</sup>) and DPHEAC (mp = 149–151°C, molecular weight = 228.25) were purchased from Sigma-Aldrich (Steinheim, Germany) and were used as received. Flax woven fabric (180 g/m<sup>2</sup>) was purchased from Libeco (Belgium) with 19 threads/cm in warp and 21 threads/cm in weft. The tensile strengths of the fabric in warp and weft, as provided by the supplier, were 835.4 and 1181 N/cm, respectively. Sodium hydroxide was purchased from Minema Chemicals (South Africa).

### Preparation of the arylated soy protein composites

In the first stage, a resin was prepared by mixing SPI with 30% TDG (w/w) for about 1 h in a 0.025M NaOH solution with a pH of about 9.5–10.<sup>14</sup> Here, TDG acted as plasticizer. To prepare the composites, flax fabrics were wetted in the SPI resin and then dried in an oven at 50°C for 24 h to get the composite sheets. The effect of the weight content of the flax fibers (20–40 wt %) on the properties of the composites was evaluated. The composites reinforced with 20, 30, and 40 wt % flax fabric were designated as S-2F, S-3F, and S-4F, respectively. These composites

were then immersed in a DPHEAC solution (0.5% w/v) for 4 h to obtain arylated composites; these were coded as S-2F-A, S-3F-A, and S-4F-A, respectively.<sup>16</sup> Subsequently, the arylated composites were taken out and placed between two steel plates fixed by binder clips to prevent dimensional instability of the arylated composites.<sup>16</sup>

### Characterizations

Fourier transform infrared (FTIR) spectra of the composites were obtained on a Spectrum 100 FTIR spectrometer (PerkinElmer, Buckinghamshire, United Kingdom) in the range 4000–650 cm<sup>-1</sup> with 8–10 mg of composite powder, which was ground manually with a pestle and mortar. Dynamic mechanical thermal analysis was performed on a dynamic mechanical analyzer (DMA8000, PerkinElmer) with a dual cantilever at a frequency of 1 Hz. The films, with dimensions of 50 × 10 mm<sup>2</sup> (Length × Width), were tested in the temperature range from 25 to 220°C with a heating rate of 2°C/min. The relaxation temperature was determined as the peak value of the loss angle tangent (tan δ). Scanning electron microscopy (SEM) images of the surfaces and cross sections of the composites were taken on an FEI Quanta 200 electron microscope (Eindhoven, The Netherlands) at an accelerating voltage of 20 kV. The cross-sectional samples for SEM characterization were prepared by freezing in liquid nitrogen before fracturing. Gold sputtering was not required for the preparation of the samples in this instrument. Thermogravimetric analysis (TGA) was carried out on dried films of approximately 5 mg at a heating rate of 10°C/min between room temperature and 700°C in a nitrogen atmosphere on a Thermogravimetric analyzer (PerkinElmer).

The tensile strength, elongation at break, and Young's modulus values of the composites were measured on an Instron 3369 testing machine at a strain rate of 10 mm/min according to ASTM D 882 (E) in the weft direction. The dimensions of the films specimens were 110 × 15 mm<sup>2</sup> (Length × Width). The clamping length for each specimen in each jaw was kept at 15 mm to prevent slippage. The fractured specimens after tensile testing were used to study the surface morphology of the arylated and nonarylated composites for qualitative studies of the

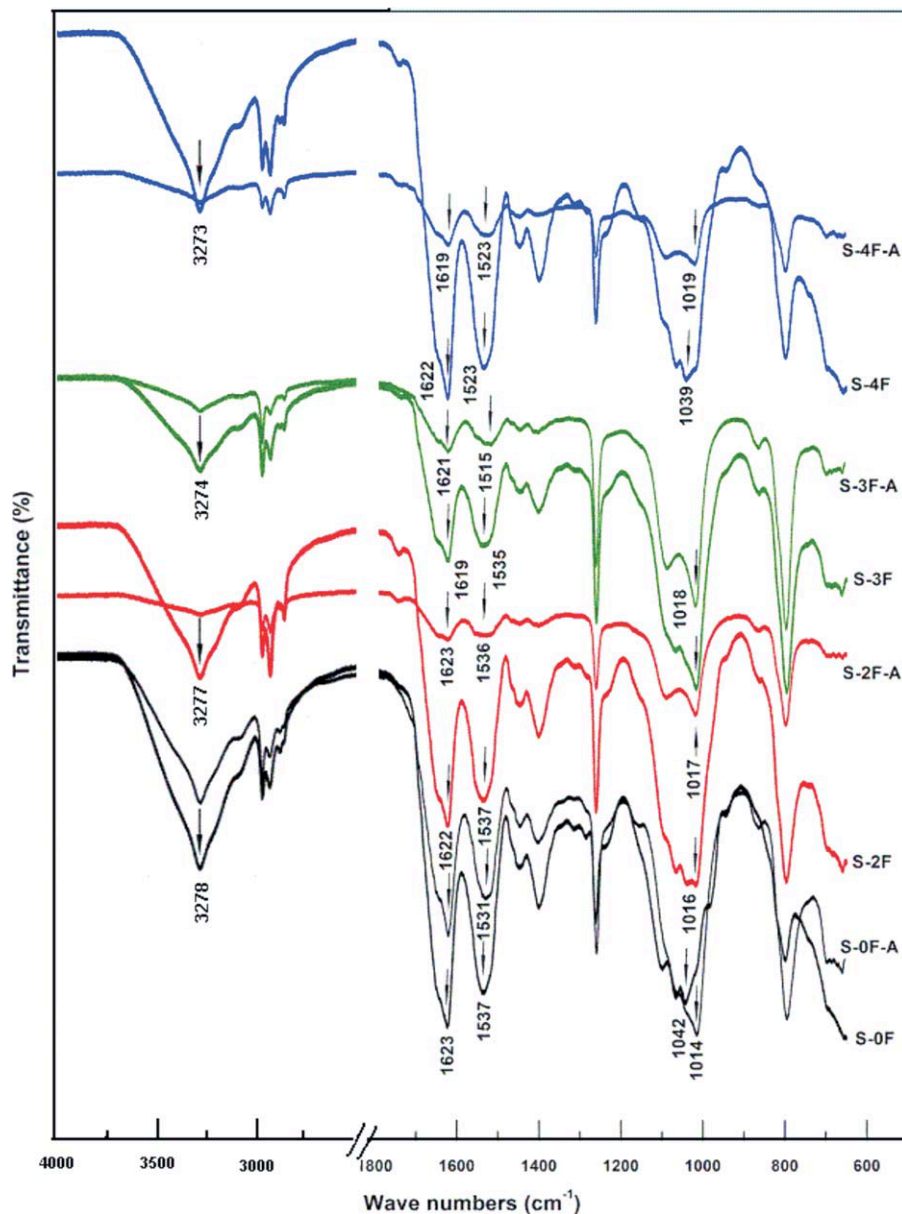


**Figure 1** FTIR spectra of the arylated and nonarylated flax-reinforced soy protein composites. [Color figure can be viewed in the online issue, which is available at [wileyonlinelibrary.com](http://wileyonlinelibrary.com).]

cracking characteristic of the arylated composites. According to the requirements for flexural testing, thicker samples (with thickness of  $3.9 \pm 0.1$  mm) of S-2F, S-2F-A, S-3F, S-3F-A, S-4F, and S-4F-A were prepared with three, five, and seven layers of flax fabric, respectively. Three-point bending tests were carried out on an Instron universal testing machine (model 3369) to determine the flexural strength. Flexural testing on a sample  $80 \times 10$  mm<sup>2</sup> in dimension was carried out in accordance with ASTM D 790 at a crosshead speed of 5 mm/min and a span length of 60 mm. An average value from five replicates of each sample was taken for each of the tests mentioned previously.

The evolution of CO<sub>2</sub> from the soy-protein-based composites during arylation was determined by a new method proposed here. The composites were preconditioned at 50°C for 24 h and weighed.  $X_1$  and  $Y_1$  represent the weights of the composites to be dipped in distilled water and a 0.5% DPHEAc solution, respectively. After immersion in distilled water for 4 h, the films were taken out and dried with paper towels to remove excess water from the surface and weighed and denoted as  $X_2$ , so  $X_2 - X_1$  is the amount of water absorbed in the SPI-based composite films. Similarly, after immersion in a 0.5% DPHEAc solution for 4 h, the films were taken out and dried with paper towels to remove excess water

**TABLE I**  
Amount of Carbon Dioxide Evolved during the Arylation of SPI Films and SPI-Flax Fiber Composites (%)

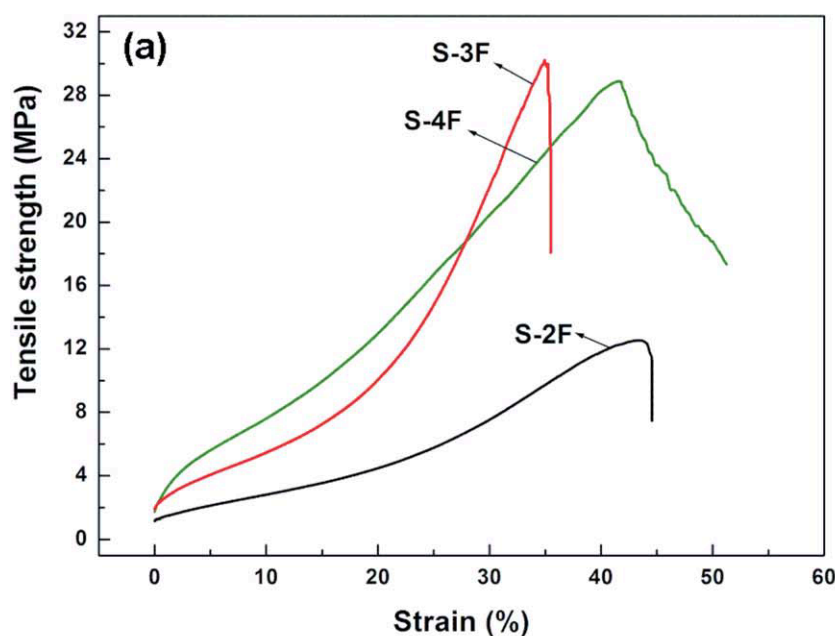
Sample	Weight (g) of $1.5 \times 1.5 \text{ cm}^2$ SPI films to be immersed		Weight (g) of SPI films taken out after 4 h from		Difference in weight (%) of SPI films taken out after 4 h from		Loss of carbon dioxide = $[(X_2 - X_1) - (Y_2 - Y_1)]$ (%)
	Water ( $X_1$ )	DPHEAc ( $Y_1$ )	Water ( $X_2$ )	DPHEAc ( $Y_2$ )	Water ( $X_2 - X_1$ ) <sup>a</sup>	DPHEAc ( $Y_2 - Y_1$ ) <sup>b</sup>	
S-0F	$0.1307 \pm 0.011$	$0.1753 \pm 0.032$	$0.6258 \pm 0.061$	$0.4152 \pm 0.135$	$378.5 \pm 7.0$	$132.2 \pm 12.5$	246.2
S-2F	$0.1813 \pm 0.017$	$0.1865 \pm 0.023$	$0.4158 \pm 0.051$	$0.3366 \pm 0.034$	$128.8 \pm 7.3$	$80.9 \pm 7.3$	47.9
S-3F	$0.1398 \pm 0.005$	$0.1427 \pm 0.012$	$0.2795 \pm 0.017$	$0.2168 \pm 0.036$	$99.6 \pm 5.0$	$51.0 \pm 12.9$	48.8
S-4F	$0.1036 \pm 0.009$	$0.1009 \pm 0.009$	$0.1998 \pm 0.014$	$0.1499 \pm 0.013$	$93.0 \pm 4.7$	$48.8 \pm 13.4$	44.6

<sup>a</sup>  $X_2 - X_1$  = Amount of water absorbed in the SPI-based composite films (%).

<sup>b</sup>  $Y_2 - Y_1$  = Amount of water absorbed in the SPI-based composite films plus the loss of carbon dioxide evolved during the arylation with DPHEAc (%).

on the surface and weighed and denoted as  $Y_2$ , so  $Y_2 - Y_1$  is the amount of water absorbed in the SPI-based composite films plus the loss of carbon dioxide evolved during arylation with DPHEAc. Thus,  $(X_2 - X_1) - (Y_2 - Y_1)$  is the loss of carbon dioxide during the arylation process.

The water uptake of the composites was evaluated according to ASTM D 570-81. The composites were preconditioned at  $50^\circ\text{C}$  for 24 h and weighed ( $W_0$ ). After immersion in distilled water for 24 h, the films were dried with paper towels to remove excess water from the surface and weighed ( $W_1$ ). The total



<b>Sample</b>	<b>Modulus (MPa)</b>
S-2F	not determined
S-3F	77.3
S-4F	114.1
S-2F-A	not determined
S-3F-A	79.5
S-4F-A	118.5

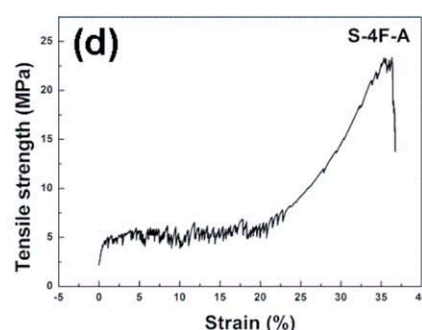
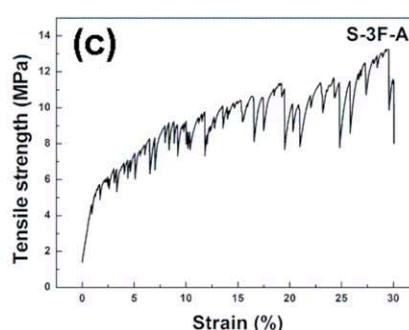
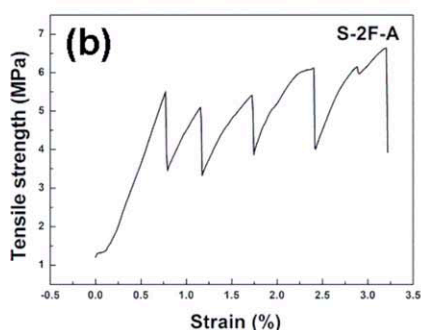


**Figure 2** Tensile stress–strain curves for (a) nonarylated and (b–d) arylated flax-reinforced soy protein composites. [Color figure can be viewed in the online issue, which is available at [wileyonlinelibrary.com](http://wileyonlinelibrary.com).]

weight gain of the composites was used to calculate the amount of water absorbed. The average value from three measurements is reported.

## RESULTS AND DISCUSSION

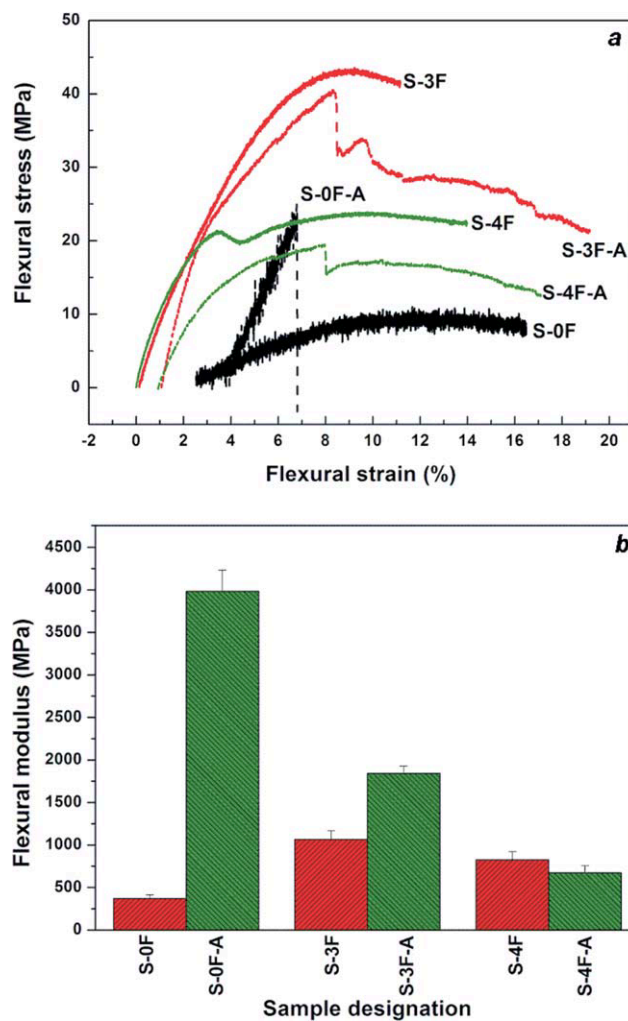
### Structural characterization and evolution of carbon dioxide

Figure 1 shows the FTIR spectra of the flax-fiber-reinforced soy protein composites. The FTIR spectra of the S-XF and S-XF-A sheets exhibited typical amide vibrations, including amide A (N–H stretching at  $3200\text{--}3400\text{ cm}^{-1}$ ), amide I (C=O stretching at  $1623\text{ cm}^{-1}$ ), and amide II and amide III (N–H bending and CN stretching around  $1537$  and  $1240\text{ cm}^{-1}$ , respectively).<sup>12</sup> Upon arylation, the amide I band of the proteins in the infrared spectra shifted to lower frequencies by  $2\text{--}4\text{ cm}^{-1}$ , whereas the amide III (N–H bending) band shifted to lower frequencies by  $6\text{--}22\text{ cm}^{-1}$ . There was decrease in the intensity of the amide A band upon arylation; this indicated a lesser degree of hydrogen bonding. The band in the composite at  $1042\text{ cm}^{-1}$  was largely due to the C–O stretching of the alcohol. There was, again, shifting of this band to lower frequencies upon incorporation of flax fabric and because of the arylation process.

Table I shows the amount of carbon dioxide evolved during arylation. The average water uptake of the soy protein films after 4 h was very high (378.4%). However, the average water uptake gradually decreased for the composites with increasing fiber content, and it was found to be 93% at 40 wt % fiber. Upon arylation for 4 h, the water uptake of the soy protein films and their composites decreased significantly. It was mentioned in an earlier article that water uptake during the arylation process is apparent water uptake because, in addition to the absorption of water, it involves the loss of  $\text{CO}_2$ .<sup>15</sup> Differences in the water uptake of nonarylated soy protein composites and the water uptake during arylation of the soy-based composites gave the loss of  $\text{CO}_2$ . The loss of  $\text{CO}_2$  was higher during the arylation of the neat SPI film, and it decreased in the range 44–48% for the soy-protein-based composites.

### Mechanical properties of the composites

The nonarylated soy protein film showed a tensile strength of 4.6 MPa with an elongation at break of 214% [not shown in Fig. 2(a)]. The tensile strength of the soy protein film reported here was low, and the percentage elongation at break was very high because of the fact that the protein films were prepared by the solution-casting method, where water also acted as plasticizer in addition to the plasticizer (TDG) that was added.<sup>11,19</sup> Figure 2(a) shows the



**Figure 3** (a) Flexural stress–strain curves and (b) flexural modulus for arylated and nonarylated flax-reinforced soy protein composites. [Color figure can be viewed in the online issue, which is available at [wileyonlinelibrary.com](http://wileyonlinelibrary.com).]

mechanical properties of the nonarylated composites. The tensile stress and modulus increased with increasing weight fraction up to 30% of the flax fabric. After that, there was decrease in the tensile stress for composites containing 40% flax fabric with increasing tensile modulus, as shown in Figure 2(a). There was decrease in the percentage elongation at break because of the flax fabric. This class of composite could be termed *damage-insensitive*.

The arylated soy protein film showed a tensile strength of 18.6 MPa with an elongation at break of 2% [not shown in Fig. 2(b)]. Hence, arylation of the soy protein led to a brittle matrix. Figure 2(b–d) shows the mechanical properties of arylated soy protein composites. For S-2F-A and S-3F-A, the maximum load on the composites was the same as that of the matrix alone; the composites continued to carry the decreasing load after the peak. The post-peak resistance was primarily provided by the

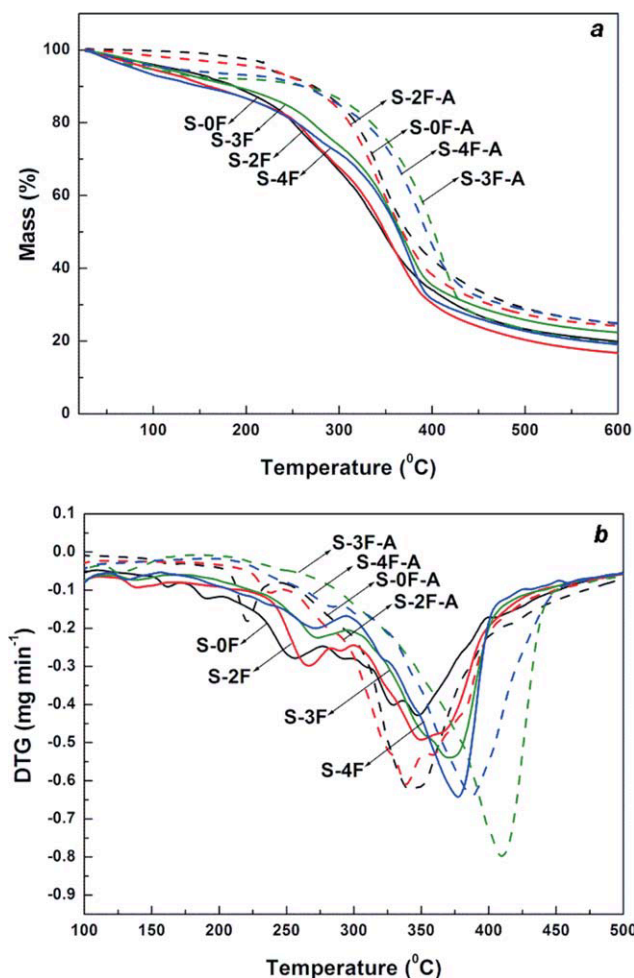


**Figure 4** (a) TGA and (b) differential thermogravimetry curves for arylated and nonarylated flax-reinforced soy protein composites. [Color figure can be viewed in the online issue, which is available at [wileyonlinelibrary.com](http://wileyonlinelibrary.com).]

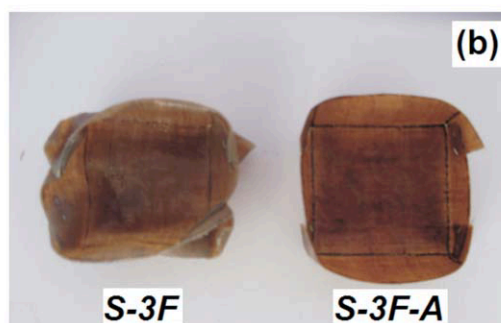
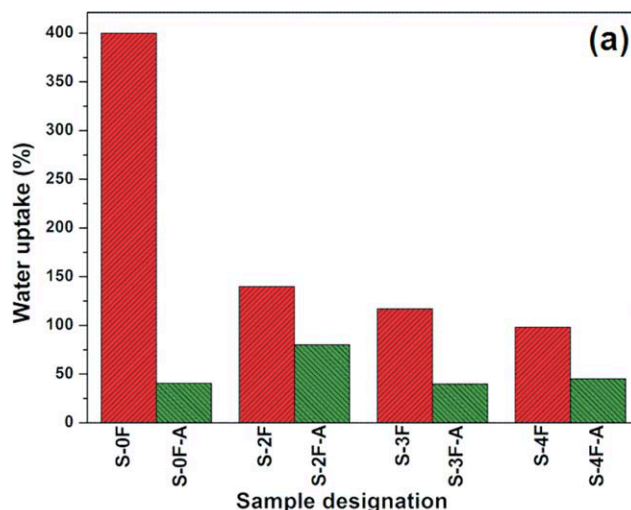
breaking of fibers from the cracked surface. Although no significant increase in the tensile strength of the arylated soy protein composite was observed, a considerable increase in the toughness of the S-3F-A composite in comparison to S-2F-A was noticed. In S-4F-A, even after the cracking of the matrix, the composite continued to bear a tensile load; the peak stress was greater than that of the matrix alone. During the inelastic range in S-4F-A, multiple cracking of the matrix, fiber debonding, and stick-slip occurred.<sup>20–22</sup> *Stick-slip* refers to the phenomenon of a spontaneous jerking motion (caused during tensile testing) that can occur while two components, such as the arylated soy protein and fabric, are sliding over each other. Thus, in the arylated composites, there was clear evidence of the stick-slip mechanism, which perhaps dominated, and it prevented easy deformation of the reinforced film.

Figure 3(a) shows the flexural stress versus flexural strain curves. It is to be mentioned here that the S-2F and S-2F-A samples could not be prepared by

**TABLE II**  
Mass Loss Values of the SPI-Flax Fiber Composites at Different Temperatures

Sample	Mass loss at different temperatures (%)			
	200°C	300°C	400°C	600°C
S-0F	11.5	34.0	66.1	79.8
S-0F-A	2.3	15.5	57.3	75.0
S-2F	13.5	32.8	70.1	83.3
S-2F-A	5.0	17.2	60.3	75.8
S-3F	11.0	26.4	64.9	79.8
S-3F-A	7.9	13.6	48.5	77.4
S-4F	13.5	28.8	68.6	80.6
S-4F-A	7.0	15.5	54.5	75.0

the solution-casting method to determine the flexural strength; hence, the results are not reported. S-3F showed highest flexural strength followed by S-4F and S-0F. Upon arylation, the composite samples again displayed the brittle-matrix behavior, as shown in Figure 2(b–d). However, the arylated composite samples showed a lower flexural strength than their nonarylated counterparts. On the contrary, the arylated composites also showed a considerable increase in the flexural modulus compared to their



**Figure 5** (a) Water uptake and (b) behavior of arylated and nonarylated flax-reinforced soy protein composites immersed in water for 24 h. [Color figure can be viewed in the online issue, which is available at [wileyonlinelibrary.com](http://wileyonlinelibrary.com).]

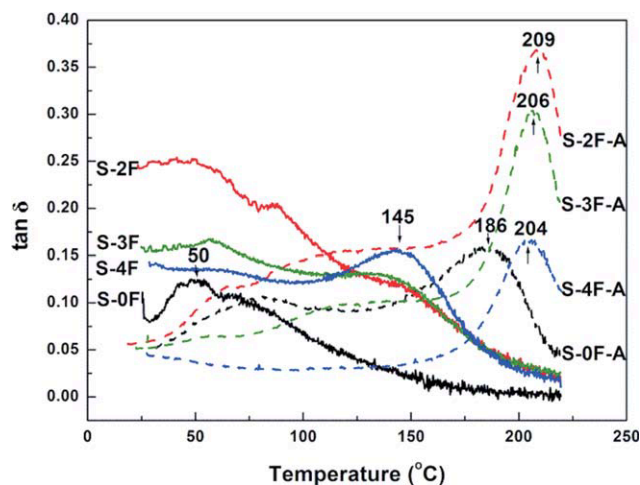


**Figure 6** Tan  $\delta$  curves of the arylated and nonarylated flax-reinforced soy protein composites. [Color figure can be viewed in the online issue, which is available at [wileyonlinelibrary.com](http://wileyonlinelibrary.com).]

nonarylated counterparts, as shown in Figure 3(b). With the reinforcement of soy protein with flax fabric, the flexural modulus of the composites decreased. From the tensile and flexural studies, 30 wt % fabric was found to be optimum.

### Thermal properties of the composites

The thermal stability of the arylated and nonarylated composites determined by TGA in a nitrogen atmosphere is shown in Figure 4. The thermal degradation of all of the nonarylated samples in the presence of TDG as a plasticizer experienced a two-stage mass loss, that is,  $T_{\max 1}$ , within the temperature range 200–300°C, and  $T_{\max 2}$ , within the temperature range 300–400°C. Here,  $T_{\max}$  represents the temperature at which the mass loss was maximum.  $T_{\max 1}$  was attributed to the loss of plasticizer, and  $T_{\max 2}$  was attributed to the degradation of soy protein and the fabric.<sup>14</sup> On the other hand, the arylated soy protein composites showed a one-stage mass loss. The  $T_{\max 1}$  peak in the arylated soy protein composites either disappeared or was of very low intensity, as reported earlier.<sup>15</sup> Table II shows the mass loss of the SPI–flax fiber composites at different temperatures. The mass loss for arylated SPI–flax fiber composites was low at all temperatures compared to the nonarylated ones; this indicated a low moisture absorption and a lesser degree of hydrogen bonding, as evidenced from the FTIR spectra (Fig. 1). More importantly, the mass loss observed in the arylated composites between 200 and 300°C also decreased;

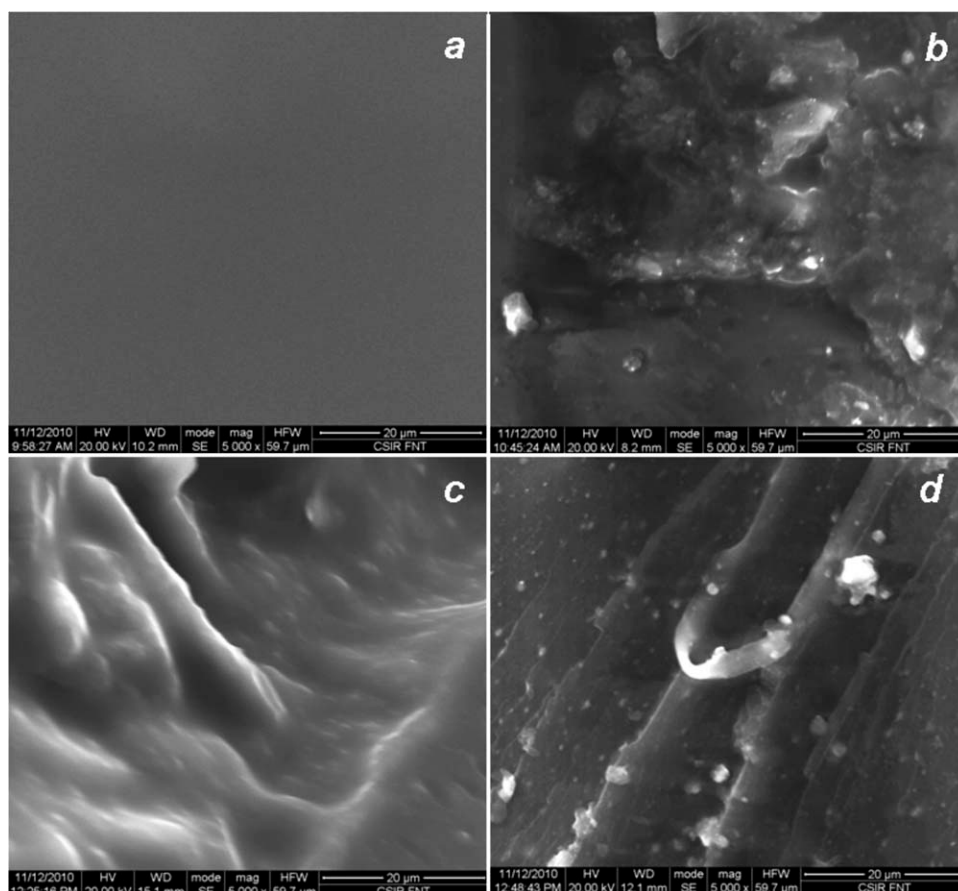


**Figure 7** (a,b) Surface and (c,d) cross section morphologies of the nonarylated and arylated flax-reinforced soy protein composites after they were subjected to tensile tests: (a,c) S-0F and (b,d) S-0F-A. The scale bar represents 20  $\mu\text{m}$ .

this suggested a single-stage mass loss for the arylated composites. The  $T_{\max 2}$  peak increased from 338°C for S-0F-A to 410°C for S-3F-A; this indicated an increased thermal stability of the composites, and again, it was found to be optimum for 30 wt % flax fabric. The char yield at 600°C for the arylated composites was higher than that for the nonarylated samples.

### Water uptake of the composites

Figure 5(a) shows the water uptake of the arylated and nonarylated composites. The arylated composites showed a low water uptake, which was similar to that reported in the literature earlier.<sup>15–18</sup> Additionally, the dimensional stability of the arylated composite, immersed in water was retained, unlike that of nonarylated ones, as shown in Figure 5(b). The lowest water uptake of S-3F-A again indicated the optimum amount of flax fabric as 30 wt %.

### Relaxation behavior

Dynamic mechanical thermal analyses of the S-XF and S-XF-A samples were carried out to provide information on the segmental motion of the protein molecules. Figure 6 shows the temperature dependence of the loss factor of the S-XF and S-XF-A films. S-0F showed  $\alpha$  relaxation around 50°C, assigned to the protein-rich domain.<sup>23</sup> Because S-0F was prepared by the solution-casting method,  $\alpha$  relaxation was much lower than what has been reported for soy protein plasticized with TDG and prepared by compression molding.<sup>14</sup> With the reinforcement of flax fabric in soy protein, there was an increase in the  $\alpha$  relaxation of the protein-rich domain to 145°C. Upon arylation, the  $\alpha$ -relaxation protein-rich domain in S-0F-A increased to 186°C, and for S-4F-A, it increased even further to 209°C. Hence, arylation of soy protein led to composites with less flexibility and higher stiffness; this has also been reported earlier in the literature.<sup>15–18</sup>

### Morphology

Figure 7 shows the morphology of the arylated and nonarylated soy protein films after they were subjected to tensile testing. As reported in the literature earlier,<sup>15–18</sup> the surface and cross-sectional morphologies of the arylated soy protein composites showed the presence of DPHM microparticles.

The surface morphology of the nonarylated composites after tensile testing showed a homogeneous surface, like S-0F, as shown in Figure 7(a). Figure 8 shows the surface morphology of the arylated soy protein composites after they were subjected to ten-

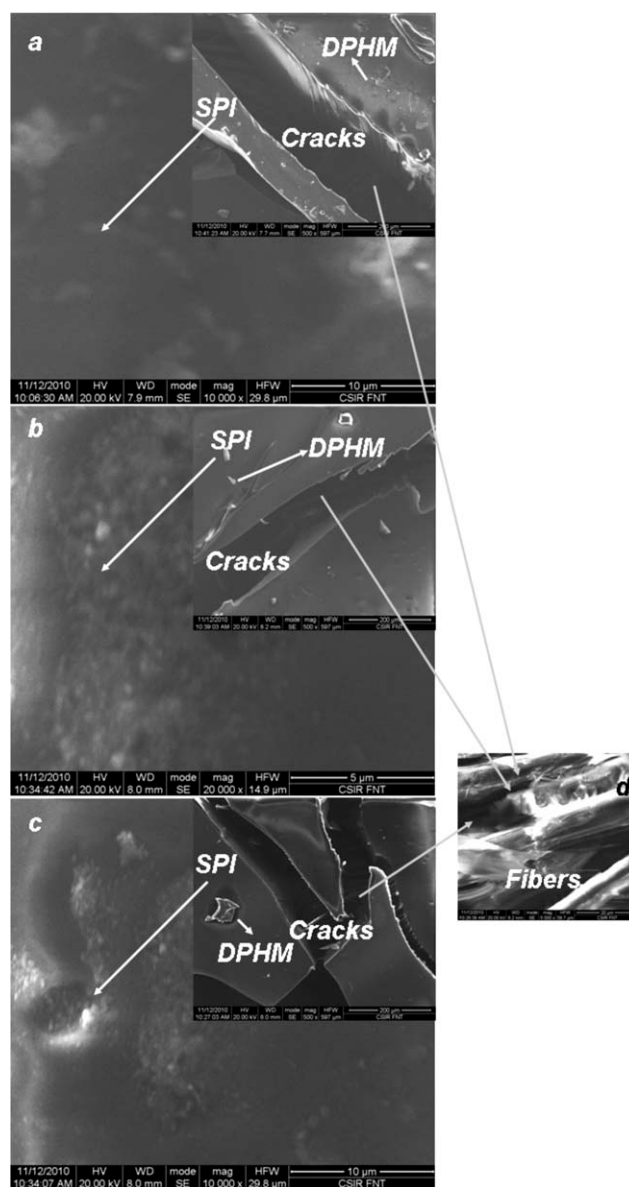


**Figure 8** Surface morphology of the arylated flax-reinforced soy protein composites after they were subjected to tensile tests: (a) S-2F-A, (b) S-3F-A, (c) S-4F-A, and (d) the morphology of flax fiber between the cracks.

sile testing. The inserts in Figure 8(a–c) represent the surface morphology of S-2F-A, S-3F-A, and S-4F-A at low magnification for visualizing the cracks in the composites after tensile tests. At high magnification, the cracks were not visible, but DPHM microparticles on the surface of the soy protein, as shown in Figure 8(a–c), and the morphology of flax fibers between the cracks, as shown in Figure 8(d), were clearly visible.

Figure 9 shows the cross-sectional morphology of the fractured surface. The presence of soy protein was visible on the surface of the flax fibers. However, upon arylation, flax fibers in S-4F-A showed complete coating of soy protein; this may have been



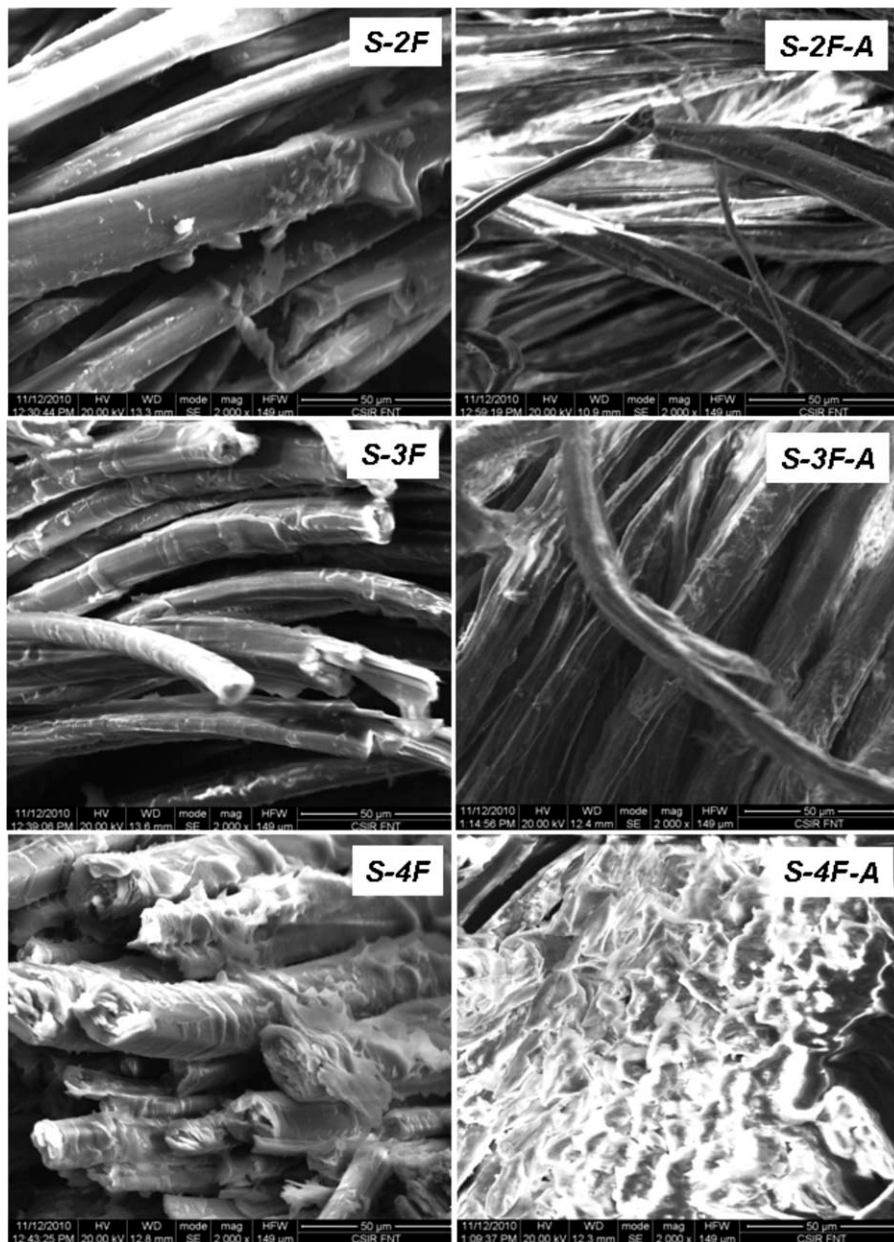


**Figure 9** SEM micrographs (cross section) of the nonarylated and aryalted flax-reinforced soy protein composites. The scale bar represents 50  $\mu\text{m}$ .

the reason for the high mechanical properties observed in the S-4F-A samples.

### CONCLUSIONS

Flax-fabric-reinforced soy protein composites, either aryalted or nonaryalted, showed better mechanical and thermal properties compared to the neat soy protein. Lower water uptake for the composites was observed at 30 wt % flax fabric. The  $\alpha$ -relaxation protein-rich domain increased upon arylation; this suggested rigidity in the aryalted soy protein composites. Results from the mechanical properties indicate the tendency of brittle-matrix behavior for the

aryalted soy protein composites; this was well confirmed by the presence of cracks on the surface of the aryalted composites, as evidenced from SEM. In the aryalted composites, there was clear evidence of a stick-slip mechanism, which perhaps dominated and, therefore, prevented easy deformation of the reinforced film.

### References

1. Lodha, P.; Netravali, A. N. *J Mater Sci* 2002, 37, 3657.
2. Lodha, P.; Netravali, A. N. *Compos Sci Technol* 2005, 65, 1211.
3. Liu, W.; Mohanty, A. K.; Askeland, P.; Drzal, L. T.; Misra, M. *Polymer* 2004, 45, 7589.

4. Chabba, S.; Netravali, A. N. *J Mater Sci* 2005, 40, 6263.
5. Huang, X.; Netravali, A. N. *Compos Sci Technol* 2007, 67, 2005.
6. Kumar, R.; Liu, D.; Zhang, L. *J Biobased Mater Bioenergy* 2008, 2, 1.
7. Lamon, J. *Compos Sci Technol* 2001, 61, 2259.
8. Ladevèze, P. *J Compos Struct* 1992, 44, 79.
9. Kuo, W. S.; Chou, T. W. *Ceram Eng Sci Proc* 1991, 12, 1556.
10. Sankari, H. *Ind Crops Prod* 2000, 11, 73.
11. Wang, L.; Kumar, R.; Zhang, L. *Frontiers Chem China* 2009, 4, 313.
12. Liu, D.; Zhang, L. *Macromol Mater Eng* 2006, 291, 820.
13. Liu, D.; Tian, H.; Zhang, L. *J Appl Polym Sci* 2007, 106, 130.
14. Kumar, R.; Wang, L.; Zhang, L. *J Appl Polym Sci* 2009, 111, 970.
15. Kumar, R.; Zhang, L. *Biomacromolecules* 2008, 9, 2430.
16. Kumar, R.; Zhang, L. *Ind Crops Prod* 2009, 29, 485.
17. Kumar, R. *Ind Eng Chem Res* 2010, 49, 3479.
18. Kumar, R.; Zhang, L. *Compos Sci Technol* 2009, 69, 555.
19. Rhim, J. W.; Lee, J. H.; Ng, P. K. W. *LWT-Food Sci Technol* 2007, 40, 232.
20. Evans, A. G.; Zok, F. W. *J Mater Sci* 1994, 29, 3857.
21. Marshall, D. B.; Cox, B. N.; Evans, A. G. *Acta Met* 1985, 33, 2013.
22. Cao, H. C.; Bischoff, E.; Sbaizero, O.; Rühle, M.; Evans, A. G.; Marshall, D. B. *J Am Ceram Soc* 1990, 73, 1691.
23. Chen, P.; Zhang, L. *Macromol Biosci* 2005, 5, 237.